

Effect of Concrete type (Normal Concrete and High- Performance Concrete) on the Corrosion Degree of Corroded Circular-Short Columns

Lubna B. Mahmood^{1*}, Assim M. Lateef²

¹CivilDepartment/Engineering College/Tikrit University/Tikrit, Iraq

Email:Lubna.b.mahmood43787@st.tu.edu.iq

²Department of Civil Engineering/College of Engineering/Tikrit University/Tikrit/ Iraq

Email:assaim77@tu.edu.iq

Article Info

Page Number:1037 - 1053

Publication Issue:

Vol 72 No. 1 (2023)

Abstract

One of the major factors in the early degradation that shortens the service life of reinforced concrete buildings is corrosion of the steel reinforcing bars. As a result, maintenance and repair expenses go up. Steel reinforcement corrosion happens gradually. In the lab, accelerated corrosion methods are often employed to mimic the natural corrosion process. Experimental work to study the effect of the type of concrete used on the degree of corrosion of longitudinal (main) reinforcing steel for short circular concrete columns. The practical program consists of four columns with dimensions of (150×1000) mm and a thickness of the clear cover of (20) mm, two of which are reference columns (High-performance concrete and Normal concrete) and two columns subject to corrosion. Tested under the influence of an axial load, the main variables adopted in the current research included the type of concrete used (Normal and High-performance concrete), The amount of reinforcing steel, the period of exposure to corrosion, the compressive strength, and other variables are constant for all models, compared with the results between all samples on the amount of weight loss of the corroded steel, the surface area of the corroded steel, and the amount of decrease in the bearing capacity of the corroded columns. During the practical test, the results showed that by using High-performance concrete, the percentage of weight loss of the reinforcing steel is reduced by (31.61) and the percentage of cross-sectional area loss is by (6.81)%, while the percentage of decrease in the bearing capacity of columns is reduced by (52.59) % in the high-performance concrete.

Keywords: High-Performance Concrete, Normal concrete, Corrosion, weight loss, Cross-Sectional Area loss, Short columns.

Article History

Article Received: 15 October 2022

Revised: 24 November 2022

Accepted: 18 December 2022

1. INTRODUCTION

Steel reinforcing bar corrosion causes RC constructions to deteriorate prematurely, Akshata Shetty (2012). As a result of corrosion, the bar loses cross-sectional area, the surrounding concrete develops fractures as a result of volumetric expansion of the corrosion product, and the bond strength is decreased, Liu, Dujian (2012). Steel corrosion also causes a decrease in bond

*Corresponding author: E-mail: lubna.b.mahmood43787@st.tu.edu.iq

strength.(X.Fu (1997), Lan Chung(2008), Yousif A.(2013), Al-Sulaimani G. J. (1990)), reducing the service life of the structure due to flexural strength Akshatha Shetty et al (2014), ductility J. Revathy et al (2009), and load-carrying capacity, J Rodriguez et al (1997), of RC element. The expense of repairing and maintaining the structures rises as a result. Steel corrosion is a severe issue, thus it has to be handled and thoroughly explored. The biggest harm is done to the in-service conditions of the RC structures by the severe corrosion of steel that occurs in the maritime environment. Steel corrosion occurs extremely slowly under natural settings; it takes a while before it causes noticeable structural damage. Francois & Arliguie (1998), Castel et al (2003), Vidal et al (2007),and Zhang et al (2009a,b; 2010)allowed RC samples to corrode spontaneously in the lab. Corrosion took place over a period of four years, and the first noticeable break on the surface of the concrete didn't develop until after another two years. After 20 years of corrosion, reasonable structural damage was attained. Research in laboratory testing cannot be conducted over such a lengthy period of time. So, in order to shorten the testing period, researchers must apply a variety of approaches to accelerate steel deterioration. They do this in the hopes that structural damage sustained during an accelerated corrosion test will be comparable to the harm brought on by steel corrosion. In general, engineers and asset managers are frequently given the research team's findings from accelerated corrosion laboratory testing so they may apply them to real-world RC structures. Engineers may permit repairs of corroding RC structures if harmful levels of steel corrosion are present or if the structures' load-bearing capacity is still sufficient if they are not relevant to such structures. Understanding how to effectively adapt (if at all relevant) the results from accelerated laboratory testing to in-service structures is important for the safety of occupants of corroding RC structures as well as to reduce expenditures from unneeded repairs. The purpose of the work is to investigate how the usage of various voltages affects steel corrosion brought on by chloride attack.

Several scholars have made significant contributions to the study of the flexural strength of corroded RC structures during the last few decades. (Wang and Liu 2010; Ma et al. 2013). The correlation between the loss of cross-section and the deterioration of flexural strength (Torres-Acosta et al. 2007; Rodriguez et al. 1997) or the loss of rebar's mass. (Yoon et al. 2000) was also studied. The majority of these investigations used an accelerated corrosion process. Other examinations also looked at the components that were taken out of already-built structures or the naturally rusted components. (Poupard et al. 2006; Vidal et al. 2007; Khan et al. 2012; Wang et al. 2013). Moreover, several researchers (Ballim and Reid 2003; Du et al. 2013) centered on the structural performance while being loaded and corroding at the same time. Some scientists are driven to develop theoretical models by combining experimental data (Coronelli and Gambarova 2004; Azad et al. 2007) or calculating the remaining flexural strength using the finite element methodology.(Kallias and Rafiq 2013). Accurately determining corrosion-induced structural performance decline is still a difficult subject.

The stiffness of RC beams may alter as a result of embedded rebars corroding. Based on load-deflection curves, several studies investigated the connection between stiffness deterioration and corrosion loss. (Cabrera 1996; Ma et al. 2014b). Castel et al. (2000) concluded that the area loss of reinforcement and stiffness degradation is related to the deterioration of the steel-concrete bond

strength. Zhang et al. (2010) suggested a mechanical model that accounts for various forms of corrosion in deflection assessment. Additional research (Torres Acosta et al. 2004; Zhong et al. 2010) examined how the loss of steel cross-section and cracking of the concrete cover affected the rigidity of beams. Malumbela et al. (2012) showed that flexural stiffness increases with increasing corrosion loss and declines at low corrosion degrees (5–8% mass loss). The investigations listed above sought to test the corroded beams using the same sort of bar. Corrosion-induced structural performance degradation is influenced by a variety of factors. It is yet unclear how corrosion in various bar types affects the flexural behavior of structures. According to certain research, the type of steel bars used determines how easily corrosive concrete cracks. In comparison to the cracked beam with deformed bars, the cracked beam with smooth bars often has fewer surface and interior cracks. (Goto 1971). Deformed bars, however, have stronger connections with concrete than smooth bars. Further experimental findings (Mohammed et al. 2001) indicated that corrosive corrosion is more likely to affect deformed bars than smooth bars. As a result, choosing steel bars is a technique for reducing the rate of corrosion in concrete beams. Structural design benefits from quantifying the impact of bar type and size on the flexural behavior of corroded beams. Sadly, thorough studies on the impact of bar type and diameter on the functionality of corroded beams are hard to come across in the accessible literature.

2. EXPERIMENTAL METHOD

2.1. *Materials*

In this study, both High-performance concrete (HPC) and normal concrete (NC) mixtures were utilized. The composition of the components used is presented in detail in "Table 1". Deformed reinforcing steel bars, measuring 6 and 8 mm in diameter, were employed. The outcomes of the tests conducted on the bars are displayed in "Table 2" and demonstrate conformity with ASTM A615 guidelines.

2.2. *Experimental Program*

Four circular short-column samples with two different types of concrete and a clear cover thickness of 20 mm. Two columns of HPC and NC were cast, and one column of each type was evaluated as part of the experimental program by being exposed to corrosion for 20 days only on longitudinal steel bars. "Table 3" contains all the information on the tested columns.

2.3. *Column specimens details*

Each specimen has a cross-section of 150 mm in diameter by 1000 mm in height, with a 20 mm clear cover. As the main longitudinal reinforcement, 6Ø8 mm steel bars were employed, together with spiral stirrups spaced 75 mm apart. "Fig.1" shows the reinforced concrete columns tested during this investigation.

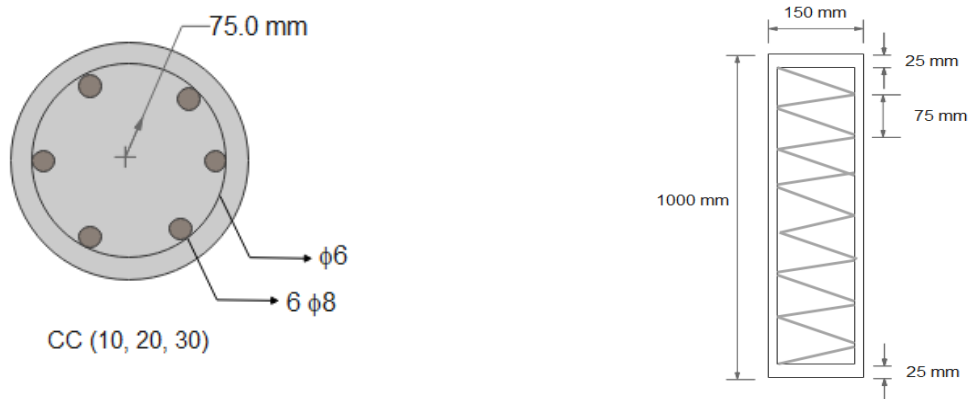


Fig. 1 The dimensions and reinforcement details of the tested columns

2.4 Molds

Plastic pipes were used for the molds, each pipe was cut to 1250 mm in length. Each mold has been cut in half all along the pipe for the purpose of re-using the molds and easily unmolding the samples after casting. Plastic pipe fittings were used to re-connect the two pieces of the molds and hold them while casting. Three pieces were used for each mold, in the top, middle, and bottom of it. A plywood base was used in the bottom of the mold placed inside the bottom pipe fitting. Fig (2) shows the used plastic pipes and the plastic fittings.



a) Cutting the molds



b) Re-connecting the molds



c) Diameter of the mold

Fig. 2 Molds details

2.5 Steel Bending Mechanism

A mechanical lathe was used to bend the steel of 6mm diameter for stirrups into spiral steel, by manual operations. A steel pipe of 90 mmdiameterwas used as a base to bend the steel over it. A smaller diameter of the steel pipe was used because the spiral stirrup gets 20 mm times bigger after removing it from the steel pipe. Fig (3) shows the lathe and the bending mechanism.



a) During Bending



b) 110 mm diameter

Fig. 3The bending mechanism

2.6 Cover Blocks and Electrical Insulation

A cover block was used as a spacer for the columns, it has been made of cement mortar of 20, mm thickness, and small plastic water pipes were used as a mold for the blocks. Small thin water pipes were used as electrical insulation, to insulate the longitudinal steel bars and stirrups for the samples that studied the corrosion for one part of the reinforcements. "Fig.4" shows the cover blocks and the electrical insulation



a) electrical insulation



b) Cover Block

Fig. 4The cover blocks and electrical insulation

2.7 Mix Design of Concrete

In this study, the material mix proportions specified in "Table 4" were utilized. To evaluate the workability of the typical concrete mix, a flow table test was conducted for HPC in accordance with ASTM C1437-01, while a slump test was performed for NC in accordance with BS1881: part 2, 1970.

2.8 Mechanical Properties

To ascertain the mechanical qualities of the concrete mix, the control specimens were mixed and poured. To evaluate the compression strength and splitting strength, three cubes of (100×100 ×100) mm for HPC, and three cubes of (150×150×150) mm for NC, were tested according to BC 1881-part 116, and three cylinders of (100×200) mm for HPC niaccordance with ASTM C496-M04, and three cylinders of (150×300) mm for NC accordance with ASTM C496-96 were tested. Table 5 displays the test results.

2.9 Absorption and Porosity

Using ASTM C 642-13, the water absorption capacity of concrete was determined. Three 100 mm cubes were taken out of the curing water after 28 days, dried in an oven at 110° C, and chilled in air dry, and then their oven-dry mass was calculated. Up until any two oven-dry weight differences were less than 0.5 percent, the oven-drying and weighing process was repeated. At that time, the ultimate mass was denoted as m_1 . After that, the samples were submerged in water for 24 hours. Before being retrieved, the mass of SSD condition (m_2) was measured by wiping away surface water with a towel. The expression in the equation below was used to compute the water absorption (W %) and was applied to the average of three samples.

$$W\% = \frac{m_2 - m_1}{m_1} \times 100$$

Where:

W%: percentage of water absorption

m_1 : mass of surface-dry specimen in the air after immersion, g

m_2 : mass of surface-dry specimen in the air after immersion, g

Since it influences the concrete's strength, durability, and transport mechanisms, such as the entrance of harmful gases and liquids, porosity is a crucial component of concrete. In this investigation, porosity was determined as the volume of permeable voids as a percentage of the solid volume in accordance with ASTM C 642-13. Three 100 mm cubes were evaluated at the age of 28 days, and the average of these samples was taken. To determine permeability voids, the water absorption test result (M_1) was used. The specimens were then cooked for five hours, cooled in water for fourteen hours, and weighed in SSD condition (M_3). A mass estimate (M_4) was also made for samples that were partially immersed and suspended in water. The equation below may be used to determine the specimens' porosity after the aforementioned mass measurements.

$$\text{Porosity \%} = \frac{M_3 - M_1}{M_3 - M_4} \times 100$$

Where:

M₁: mass of oven-dried specimen in air, g

M₃: mass of surface-dry specimen in the air after immersion and boiling, g

M₄: apparent mass of specimen in water after immersion and boiling,

2.10 Corrosion Cell

According to Li et al., 2018, the accelerated corrosion technique was employed in this study for 20 days at a current density of 1 mill ampere per cubic centimeter. The specimens in the corrosion basin were supplied with electricity using a dual power supply model (PS 303-2) with a maximum current of 3A and a voltage of 30V. The sample size was taken into consideration while delivering the electricity, which was 1.43 A (surface area for longitudinal steel bars). The cathode electrode under each column was a stainless steel plate, while the anode electrode was made up of longitudinal steel bars, often eight per column. 5% of pure salt (NaCl) was used, based on the basin's volume. A corroded column and the corrosion cell in use are shown in Figure 5 respectively.



a) the corrosion cell during operation



b) corroded columns

Fig.5:Corrosion Process

Table 1 Description of Materials

Material	Descriptions
	HPC
Cement	Mass Factory's Type I ordinary Portland cement is consistent with Iraqi Specification No. 5/1984.

Quartz Sand	Quartz sand with a maximum size of 600 μ m and compatible with the B.S. specification No.882/1992.
Silica Fume	A highly active pozzolanic substance made up of very small, spherical particles known as micro-silica (BASF MasterRoc MS610) is compatible with the ASTM C1240-03.
Super Plasticizer	The admixture BASF MasterGlenium 51 (Advanced Polycarboxylate Super Plasticizer) was used and compatible with the ASTM C494, 2013.
Water	pristine tap water (used for mixing and curing)
Steel Bars	Deformed steel bars with a diameter of 8 and 6 mm
NC	
Cement	The Ordinary Portland cement (Type I) used in this study was manufactured by Mass factory and was in compliance with Iraqi specification No.5/1984.
Coarse Aggregate	The gravel had a maximum nominal size of 12.5 mm and met the standards outlined in the Iraqi specification No.45/1984.
Fine Aggregate	Fine aggregate compatible with the Iraqi specification No.45 /1984.
Water	pristine tap water (used for mixing and curing)
Steel Bars	Deformed steel bars with a diameter of 8 and 6 mm

Table 2 Test Results of Steel Bar Reinforcement

Bar diameter (mm)	Measured diameter (mm)	Yield stress f_y (MPa)	Ultimate stress f_u (MPa)	Elongation %
6	5.6	430	568.80	6.1
8	8	450	625.88	7.3

Table 3 General information and the tested columns' variables

Column Symbol	Type of Column	Type of Concrete
H.R.20	Control Column	HPC
N.R.20	Control Column	NC
H.C.L.20	Corroded Column	HPC
N.C.L.20	Corroded Column	NC

Table 4 Mix Proportion

HPC					
Ingredient	Cement	Quartz Sand	Silica	SP %	W/C ratio
Quantities (Kg/m ³)	1000	1000	100	1.8	0.22
NC					

Ingredient	Cement	Sand	Gravel	Water	W/C ratio
Quantities (Kg/m ³)	378.22	797	910	171.69	0.453

Table 5 Concrete Mix Mechanical Characteristics

Compressive Strength f_{cu} (MPa)	Splitting Tensile Strength f_{ct} (MPa)	Absorption (%)	Porosity (%)
HPC			
80	7	0.8	0.5
NC			
24	3	3.98	4.5

2.8 Columns Test

Initially, the column to be tested is positioned in the designated location of the testing device. Subsequently, the LVDT (Linear Variable Differential Transformer) is affixed adjacent to the column. To simulate a linear load, a force was applied to the specimens via a cylindrical roller. The specimens were also loaded axially through a support plate. The load was gradually increased, with measurements recorded every 5.0 KN until the point of failure. The axial deformation of the columns in response to the load was monitored using a vertical LVDT positioned at the top base of the testing equipment, which could move up and down. Longitudinal strains were measured using a strain gauge. The measurement process for each load increase is illustrated in Figure 6.



Fig.6: Testing Device

2.9 Corrosion Determination

Following the testing and breaking of the damaged columns corroded reinforcing steel bars were cleaned using kerosene oil to eliminate any rust particles. The weight loss method and loss in the cross-sectional area were utilized to determine the corrosion losses for the steel bars, as outlined by Li et al. (2018) and presented in Table 6.

2.9.1 Percentage of Weight Loss

The weight loss method involves weighing the steel bars both prior to and following the corrosion process. The weight loss percentage (%) is then calculated utilizing the following equation:

$$\omega\% = \frac{w_1 - w_2}{w_1} * 100\%$$

In the equation, w1 and w2 represent the weights of the steel bars before and after corrosion, respectively.

2.9.2 Sectional Area Loss

As outlined by Li et al. (2018), the sectional area loss for the steel bars before and after the corrosion process was determined by measuring the average diameter at six different locations on each steel bar. The area of each average diameter was then calculated.

3. RESULTS AND DISCUSSION

The effects of the concrete type on corrosion degree by estimated weight loss % and sectional area loss % were tested on control and corroded reinforced concrete column specimens (see Figure 6) during the experimental program. The test outcomes are displayed in "Table 6".



a) H.R.20



b) N.R.20



Fig.6: Tested Samples

3.1 Ultimate Loads

All column specimens were tested until failure, and the ultimate loads of the tested columns were recorded and presented in Table 6. The results indicate that the ultimate loads for the corroded samples of both HPC and NC decreased by approximately 25.25% and 29.79%, respectively, when compared to the control columns. This reduction in load-bearing capacity is attributed to the damage caused by corrosion, as illustrated in Figure 7.

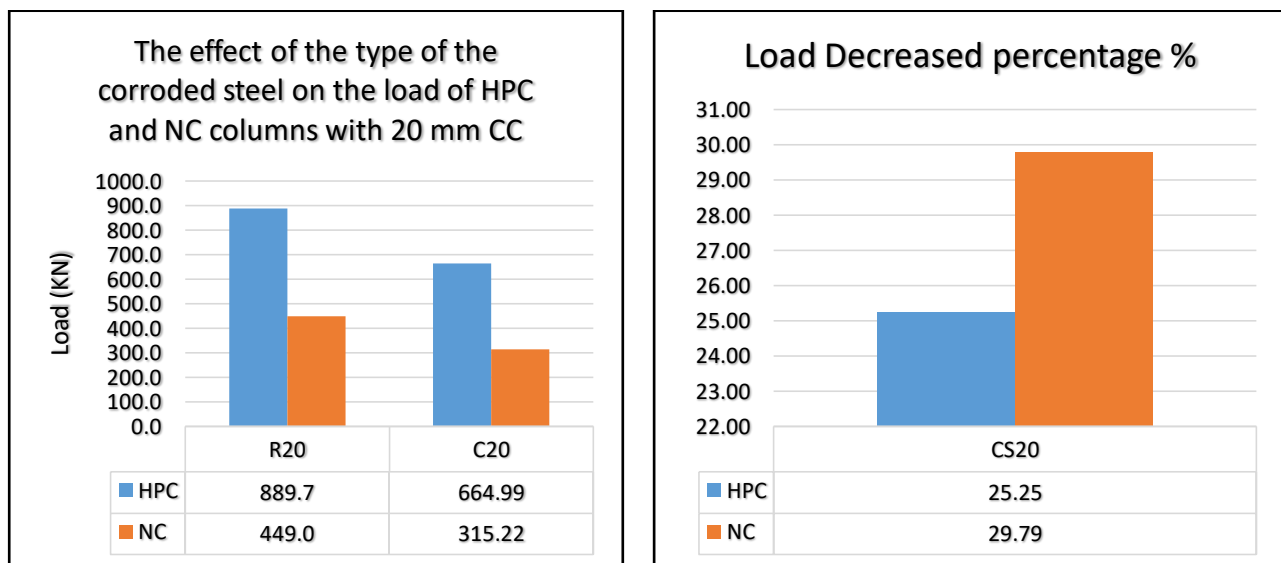


Fig.7: Load Decreasing Results

3.2 Percentage of Weight Loss

The weight loss percentages of the longitudinal reinforcement steel bars after the corrosion process for HPC and NC decreased by (11.82 and 14.29) % respectively, compared to the control columns as shown in Fig.8. The weight of steel in the corroded columns was also recorded and presented in "Table 6".

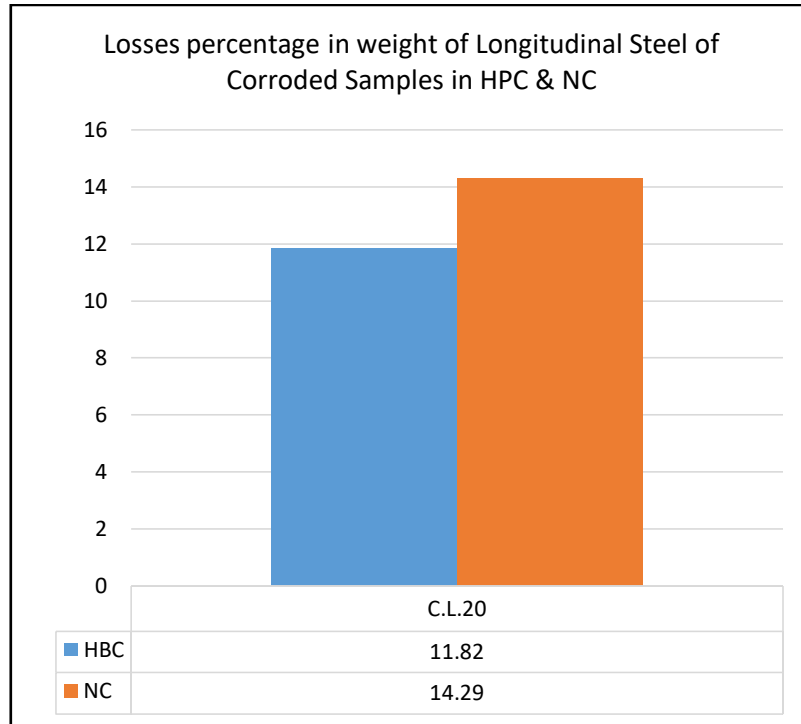


Fig.8:Losses of the steel bar’s weight

3.3 Losses in Cross-Sectional Area

As presented in "Table6", the sectional area of the steel bars after the corrosion process decreased by (64.0 and 68.36) % for HPC and NC columns, respectively, compared to the control columns.and as shown in Fig.9the cross-sectional loss percentage decreases with respect to the control columns.Fig. 9shows a corroded steel bar.

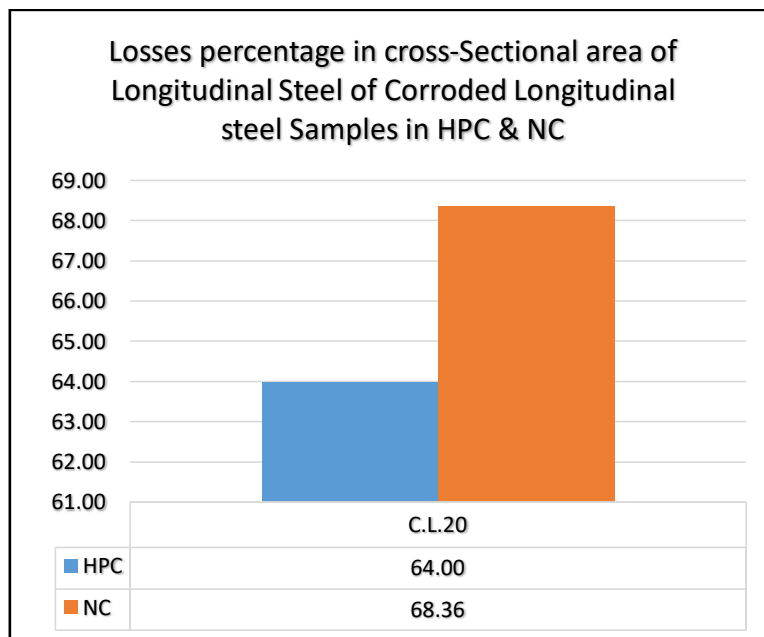


Fig.9:Losses in cross-sectional area



Fig.10:Corroded Steel Bar

Table 6 Column Specimens Test's Results

Column Symbol	Loads (KN)	Steel Bar Weight (g)	Steel bar Sectional Area (mm ²)
H.R.20	889.66	195.00	50.265
N.R.20	448.95	195.00	50.265
H.C.L.20	664.99	171.96	18.10
N.C.L.20	315.22	167.13	15.904

4. CONCLUSIONS

From the experimental work conducted, the following conclusions can be inferred:

1. Firstly, the results of the ultimate loads of the control columns showed that the bearing capacity of the high-performance concrete columns was higher by (50.463)% than the normal concrete columns, and this is due to the characteristics of the high-performance concrete, which is distinguished from the normal concrete by its high resistance.
2. The results of the ultimate loads of corrosion-prone columns also showed that the decrease in the column's bearing capacity was less by (52.598)% in the high-performance columns compared to the normal concrete columns, and this indicates that the effect of corrosion on the bearing capacity of high-performance concrete samples is less than its effect on the normal concrete.
3. The accelerated corrosion process led to a weight loss in steel bars of (11.82)% for HPC and (17.285)% for NC, compared to the control columns. Moreover, the weight loss in the HPC columns was (31.617)% lower than that in the NC columns.
4. As for the loss in the cross-sectional area of longitudinal steel bars was about (64.00 and 68.36) % for HPC and NC respectively, whereas, the percentage of loss in the cross-

sectional area of steel for the HPC column was less by (6.81) % than the normal concrete column.

5. Also, the results of the porosity and water absorption tests showed that the percentage of porosity and water absorption in HPC is lower by (88.889 and 79.899) %, respectively, compared to the normal concrete.
6. From the analysis of the results and the comparison of the NC and HPC, as expected, it was found that the effect of corrosion on the HPC is less than the effect on the NC, as the low percentage of pores and water absorption in the HPC was a clear reason for reducing the rate of corrosion, as the pores are the inlet that the water and corrosive materials take to reach the reinforcing steel and interact with it, and this causes corrode and increase its size, thus cracking and smashing the structural members, and in advanced cases, it causes a fall in the concrete cover, which leads to the failure of the structural member. The NC column showed higher losses in the weight of the reinforcing steel and in its cross-sectional area, and thus a decrease in the bearing capacity of the column.

NOMENCLATURE

Abbreviation	Description
HPC	High-Performance Concrete
NC	Normal Concrete

REFERENCES

1. ACI 318M-14, (2014), Building Code Requirements for Structural Concrete (ACI 318M- 14) and Commentary. An ACI Standard, Reported by ACI Committee 318.
2. ACI Committee 211, (2002), Standard Practice for Selecting Proportions for Normal, Heavyweight, and Mass Concrete (ACI 211.1-91), American Concrete Institute.
3. Akshata Shetty, Katta Venkataramana and Indranil Gogoi “Performance Evaluation of Rebar in Accelerated Corrosion by Gravimetric Loss Method,” International journal of earth sciences and engineering, ISSN 0974-5904, Volume 05, No. 01 February 2012, P.P. 154-159.
4. Akshatha Shetty et al “Effect of corrosion on flexural bond strength,” J. Electrochem. Sci. Eng. 4(3) (2014) 123-134; doi: 10.5599/jese.2014.0052
5. Al-Sulaimani G. J., Kaleemullah M., Basunbul I.A., and Rasheeduzzafar: “Influence of corrosion and cracking on bond behavior and strength of reinforced concrete members.” ACI Structural Journal, Vol. 87(2), 1990, pp. 220–231.
6. ASTM A615/A615M-09. Standard Specifications for Deformed and Plain Carbon-Steel Bars for Concrete Reinforcement.
7. ASTM C 494/C494M-17, " Standard Specifications for Chemical Admixtures for Concrete".
8. ASTM C109/C 109M -99. Standard Test Method for Compressive Strength of Hydraulic Cement Mortars.
9. ASTM C1240 -03, " Standard Specifications for Use of Silica Fume as a Mineral Admixture in Hydraulic –Cement Concrete, Mortar, and Grout"

10. ASTM C1437, (2001), "Standard Test Method for Flow of Hydraulic Cement Pastes and Mortars of Plastic Consistency".
11. ASTM C348. Standard Test Method for Flexural Strength of Hydraulic–Cement Mortars. Iraqi Specifications, No.5/1984. Portland cement.
12. ASTM C642-13. Standard Test Method for Density, Absorption, and Voids in Hardened Concrete.
13. Azad, A. K., Ahmad, S., and Azher, S. A. (2007). "Residual strength of corrosion-damaged reinforced concrete beams." *ACI Mater. J.*, 104(1), 40–47.
14. B.S.882, (1992) "Specifications for Aggregates from Natural Sources for Concrete " British Standards Institute.
15. Ballim, Y., and Reid, J. C. (2003). "Reinforcement corrosion and the deflection of RC beams—an experimental critique of current test methods." *Cem. Concr. Comp.*, 25(6), 625–632
16. BS 1881, Part 116, (1989), "Method for Determination of Compressive Strength of Concrete Cubes ", British Standards Institution, 3pp.
17. Cabrera, J. G. (1996). "Deterioration of concrete due to reinforcement steel corrosion." *Cem. Concr. Comp.*, 18(1), 47–59.
18. Castel, A, Vidal, T, Francois, R & Arliguie, G 2003 "Influence of steel–concrete interface quality on reinforcement corrosion induced by chlorides," *Magazine of Concrete Research*, 55(2): 151–159
19. Castel, A., François, R., and Arliguie, G. (2000). "Mechanical behavior of corroded reinforced concrete beams. Part 1: Experimental study of corroded beams." *Mater. Struct.*, 33(9), 539–544
20. Coronelli, D., and Gambarova, P. (2004). "Structural assessment of corroded reinforced concrete beams: modeling guidelines." *J. Struct. Eng.*, 10.1061/(ASCE)0733-9445(2004)130:8(1214), 1214–1224.
21. Dr. J Rodriguez et al "Load carrying capacity of concrete structures with corroded reinforcement," *Construcion and Building Materials*, Vol. II, No. 4. pp. 239-248, 1997.
22. Du, Y. G., Cullen, M., and Li, C. (2013). "Structural performance of RC beams under simultaneous loading and reinforcement corrosion." *Constr. Build. Mater.*, 38, 472–481.
23. Francois, R & Arliguie, G 1998."Influence of service cracking on reinforcement steel corrosion," *Journal of Materials in Civil Engineering*, 10(1): 14–20.
24. Goto, Y. (1971). "Cracks formed in concrete around deformed tension bars." *ACI J.*, 68(4), 244–251.
25. J. Revathy et al "Effect of Corrosion Damage on the Ductility Performance of Concrete Columns," *American J. of Engineering and Applied Sciences* 2 (2): 324-327, 2009 ISSN 1941-7020.
26. Kallias, A. N., and Rafiq, M. (2013). "Performance assessment of corroding RC beams using response surface methodology." *Eng. Struct.*, 49, 671–685.
27. Khan, I., François, R., and Castel, A. (2012). "Structural performance of a 26-year-old corroded reinforced concrete beam." *Eur. J. Env. Civil Eng.*, 16(3–4), 440–449.
28. Lan Chung(2008) "Bond strength prediction for reinforced concrete members with highly corroded reinforcing bars," *Cement and Concrete composites* 30(2008), pp 603-611

29. Li H, Li B, Jin R, Li S, & Yu JG (2018). Effects of sustained loading and corrosion on the performance of reinforced concrete beams. *Construction and Building Materials*, 169, 179-187.
30. Ma, Y., Wang, L., Zhang, J., Xiang, Y., Peng, T., and Liu, Y. (2014b). "Hybrid uncertainty quantification for probabilistic corrosion damage prediction for aging RC bridges." *J. Mater. Civ. Eng.*, 10.1061/(ASCE)MT.1943-5533.0001096, 04014152.
31. Ma, Y., Zhang, J., Wang, L., and Liu, Y. (2013). "Probabilistic prediction with Bayesian updating for strength degradation of RC bridge beams."
32. Malumbela, G., Moyo, P., and Alexander, M. (2012). "Longitudinal strains and stiffness of RC beams under load as measures of corrosion levels." *Eng. Struct.*, 35, 215–227.
33. Mohammed, T., Otsuki, N., Hisada, M., and Shibata, T. (2001). "Effect of crack width and bar types on corrosion of steel in concrete." *J. Mater. Civ. Eng.*, 10.1061/(ASCE)0899-1561(2001)13:3(194), 194–201
34. Poupard, O., L'Hostis, V., Catinaud, S., and Petre-Lazar, I. (2006). "Corrosion damage diagnosis of a reinforced concrete beam after 40 years natural exposure in marine environment." *Cem. Concr. Res.*, 36(3), 504–520.
35. Rodriguez, J., Ortega, L. M., and Casal, J. (1997). "Load carrying capacity of concrete structures with corroded reinforcement." *Constr. Build. Mater.*, 11(4), 239–248.
36. Tiejun Liu, Dujian Zou, Jun Teng "Experimental investigation on the dynamic properties of RC structures affected by reinforcement corrosion," Harbin Institute of Technology, Shenzhen, 518055, china, Lisboa 2012
37. Torres-Acosta, A. A., Fabela-Gallegos, M. J., Munoz-Noval, A., Vázquez- ~ Vega, D., Hernandez-Jimenez, J. R., and Martínez-Madrid, M. (2004). "Influence of corrosion on the structural stiffness of reinforced concrete beams." *Corrosion*, 60(9), 862–872.
38. Torres-Acosta, A. A., Fabela-Gallegos, M. J., Munoz-Noval, A., Vázquez- ~ Vega, D., Hernandez-Jimenez, J. R., and Martínez-Madrid, M. (2004). "Influence of corrosion on the structural stiffness of reinforced concrete beams." *Corrosion*, 60(9), 862–872.
39. Vidal, T, Castel, A & Francois, R 2007. "Corrosion process and structural performance of a 17-year-old reinforced concrete beam stored in a chloride environment," *Cement & Concrete Research* 37: 1551–1561.
40. Vidal, T., Castel, A., and François, R. (2007). "Corrosion process and structural performance of a 17-year-old reinforced concrete beam stored in chloride environment." *Cem. Concr. Res.*, 37(11), 1551–1561.
41. Wang, L., Ma, Y., Zhang, J., and Liu, Y. (2013). "Probabilistic analysis of corrosion of reinforcement in RC bridge considering fuzziness and randomness." *J. Struct. Eng.*, 10.1061/(ASCE)ST.1943-541X.0000738, 1529–1540
42. Wang, X. H., and Liu, X. L. (2010). "Simplified methodology for the evaluation of the residual strength of corroded reinforced concrete beams." *J. Perform. Constr. Facil.*, 10.1061/(ASCE)CF.1943-5509.0000083, 108–119.
43. X.Fu and DLL Chung "Effect of corrosion on the bond between concrete and steel bar," *Composite Materials Research Laboratory, State university of New York. Res.*, 27: 1811-1815.DOI: 10.1016/S0008-8846(97)00172-5,1997.

44. Yoon, S., Wang, K., Weiss, W. J., and Shah, S. P. (2000). "Interaction between loading, corrosion, and serviceability of reinforced concrete." *ACI Mater. J.*, 97(6), 637–644
45. Yousif A. Mansoor " The Reinforcement Bond Strength Behavior under Different Corrosion Condition," *Research Journal of Applied Sciences, Engineering and Technology* 5(7): 2346-2353, 2013
46. Zhang, R, Castel, A & Francois, R 2009a " Serviceability limit state criteria based on steel–concrete bond loss for corroded reinforced concrete in chloride environment," *Materials & Structures*, 42(10): 1407–1421.
47. Zhang, R, Castel, A & Francois, R 2009b "The corrosion pattern of reinforcement and its influence on serviceability of reinforced concrete members in chloride environment," *Cement & Concrete Research*, 39(11): 1077–1086.
48. Zhang, R, Castel, A & Francois, R 2010. "Concrete cover cracking with reinforcement corrosion of RC beam during chloride-induced corrosion process," *Cement& Concrete Research*, 40(3): 415–425.
49. Zhang, R. J., Castel, A., and Francois, R. (2010). "Effect of steel corrosion pattern on RC beam performance." *Proc. Inst. Civ. Eng.: Constr. Mater.*, 163(2), 97–108.
50. Zhong, J., Gardoni, P., and Rosowsky, D. (2010). "Stiffness degradation and time to cracking of cover concrete in reinforced concrete structures subject to corrosion." *J. Eng. Mech.*, 10.1061/(ASCE)EM.1943-7889 .0000074, 209–219.